

This is the accepted manuscript made available via CHORUS. The article has been published as:

Crystalline diborane at high pressures

Kazutaka Abe and N. W. Ashcroft

Phys. Rev. B **84**, 104118 — Published 19 September 2011

DOI: [10.1103/PhysRevB.84.104118](https://doi.org/10.1103/PhysRevB.84.104118)

Crystalline diborane at high pressures

Kazutaka Abe¹ and N. W. Ashcroft²

¹*Research Institute of Electrical Communication, Tohoku University,
2-1-1 Katahira, Aoba-ku, Sendai, Miyagi 980-8577, JAPAN*

²*Laboratory of Atomic and Solid State Physics, Cornell University,
Clark Hall, Ithaca, New York 14853-2501, USA*

Abstract

High pressure ground-state phases of crystalline diborane (B_2H_6) and their stability against decomposition into B and H are investigated by calculations within density functional theory. Although B_2H_6 is thermodynamically unstable to phase separation into B and H in the intermediate pressure range, it is re-stabilized beyond 350 GPa. The candidate structures are then $Pbcn$ and $Cmcm$, though at the level of the harmonic approximation the latter has some imaginary-frequency phonons. Both structures are metallic with quite high density of states at the Fermi energy. An estimate of superconducting transition temperature T_c is carried out for the $Pbcn$ structure by using the extended McMillan formula, and the resulting T_c reaches around 100 K.

PACS numbers: 74.62.Fj, 74.70.Ad, 71.30.+h

Compressing hydrogen-rich compounds may yield new pathways in approaches to attaining a metallic state of hydrogen itself at high pressures¹⁻³. The advantage of treating hydrides rather than pure hydrogen lies in the idea that because of possible chemical pre-compression the metallization of hydrides tends to require lower pressure than those expected for hydrogen. An example of recent interests is SiH₄, whose properties at megabar pressures have been well investigated theoretically⁴⁻⁷ and experimentally⁸⁻¹⁰. Save for CH₄ the hydrides of Group 14 are not thermodynamically stable, though they are kinetically persistent. Although a stable metallic phase of SiH₄ has not been found up to 200 GPa as yet⁸⁻¹⁰, it is expected that SiH₄ metallizes between 200 and 300 GPa^{5,10}. This predicted pressure is lower than that of the equivalent for hydrogen. Indeed, hydrogen is known to be insulating or even semiconducting at least up to 320 GPa under static compression¹¹⁻¹³.

One of the interests in the metallic form of hydrogen and its metallic compounds is the possibility of high- T_c superconductivity^{2,3,14}. The motivation tempts one to investigate the hydrides of the first-row p elements because of their low masses and strong electron-ion interactions. A drawback in considering these hydrides is that the metallization pressure still tends to be high, and indeed may even be higher than in hydrogen. For example, this tendency is experimentally observed for CH₄, which is not metallic at least up to 300 GPa^{15,16}. Also, the common high-hydride NH₃ is not predicted to be metallic below 500 GPa from recent first-principles calculations¹⁷. These observations are of relevance and specifically within a view of the tendency towards a localized character of $2p$ electrons.

Yet, as one possible exception, it may be worth examining the light element system B₂H₆, which was recently compressed up to 50 GPa at room temperature with three new solid phases then being found from analysis of optical measurements¹⁸. Since BH₃ tends to form B₂H₆, B₂H₆ can be considered the simplest compound in extensive boron hydrides, which are known to possess the curious valence structure, namely, three-center bond^{19,20}. As with most Group-14 hydrides, B₂H₆ has a positive heat of formation but is kinetically stable at normal conditions. One of the more noticeable properties of B₂H₆ is its notably high polarizability. The Goldhammer-Herzfeld (GH) criterion²¹, which is based on the Clausius-Mossotti equation, then predicts that an insulator-to-metal transition should take place when the volume per molecule v_M satisfies $v_M = (4\pi/3)\alpha$ for high symmetry structures, where α is the static linear dipole-polarizability of a single molecule. According to our estimate from the density functional perturbation theory (DFPT)²², the value of α of a

B_2H_6 molecule is 6.14 \AA^3 (or $41.4 a_0^3$) when the largest component is taken. The GH relation then gives $r_s = 1.51$ for the onset of metallization. Here r_s is the standard linear measure of inverse average valence electron density. For the sake of comparison, a similar analysis can be carried out for H_2 and NH_3 , whose largest components of α are 1.03 and 2.56 \AA^3 , respectively. Then, from the GH relation, the metallization density of H_2 is $r_s = 1.51$, and that of NH_3 is $r_s = 1.29$. These densities of B_2H_6 , H_2 , and NH_3 roughly correspond to 90, 120, 150 GPa, respectively, from our density functional calculations. As expected, the GH criterion is insufficiently accurate to predict the absolute value of the transition density, for as noted experimentally hydrogen remains non-metallic even around 320 GPa^{11–13}. However, the criterion strongly suggests that B_2H_6 may metallize at a lower pressure and therefore may also have more of a tendency to reveal a highly metallic character than will H_2 and NH_3 .

Accordingly, in this paper, we investigate B_2H_6 at high pressures by theoretical means. Calculations are carried out by using density-functional theory within the generalized gradient approximation (GGA)²³. Initially the system is taken as static. We have used planewave basis sets and the projector augmented-wave method²⁴, and have utilized VASP to implement the computations²⁵. The number of \mathbf{k} -points is taken to be $n_k = (40\text{\AA})^3/v_{\text{cell}}$, where v_{cell} is the volume of the unit cell, with a Fermi-distribution smearing of the temperature of $k_{\text{B}}T = 0.1 \text{ eV}$. The cutoff energy has been set at 950 eV for pseudopotential whose outermost cutoff radii are taken to be 0.582 \AA for B and 0.423 \AA for H.

In the present study, we mainly investigate structures where the primitive cell contains at most two B_2H_6 molecules ($Z = 2$). In searching for stable structures, we first set up several trial structures at low density, $r_s \sim 2.2$. Then, by increasing the density step by step from $r_s \sim 2.2$ to $r_s \sim 1.18$, we have also examined the phases at megabar pressures. The enthalpy of candidate structures obtained in this manner is shown, per valence electron, in Fig. 1, together with the enthalpy of a disproportionated system consisting of B and H phases. Looking ahead, we will find that some of the hydrogen related phonons have energies as high as 3000 cm^{-1} (or about 0.37 eV); the enthalpy differences in Fig. 1 are characterized by $\sim 0.02 \text{ eV}$. So far as the static B_2H_6 system is concerned, the lowest-enthalpy structure transforms according to $P2_1/c \rightarrow Pna2_1 \rightarrow P2_1/m \rightarrow Pbcn$ ³³. It turns out, however, that the disproportionated system has lower enthalpy than the B_2H_6 phases from about 40 to 350 GPa. Thus, B_2H_6 crystal becomes unstable as the pressure is increased, but is re-stabilized

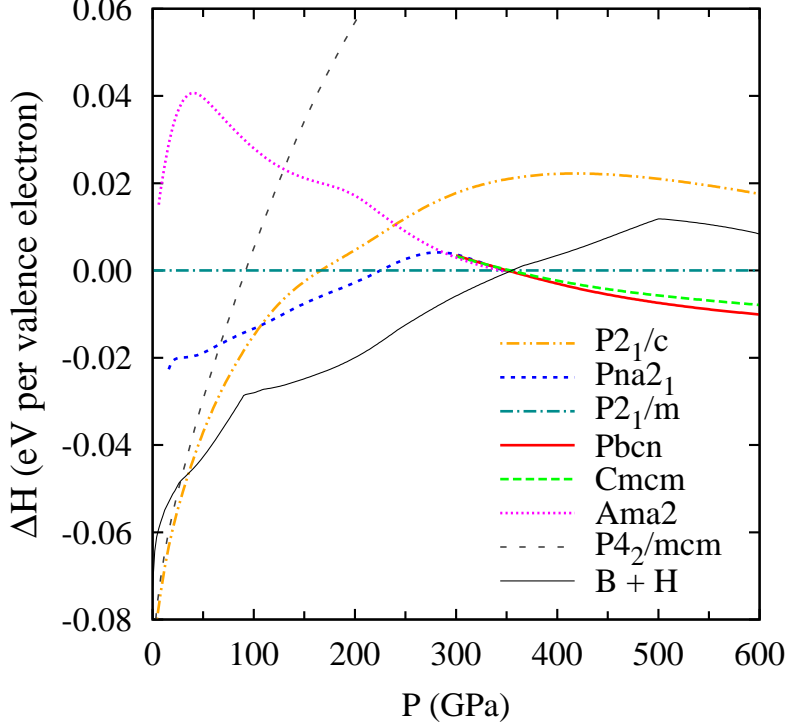


FIG. 1: (color online). The ground-state enthalpy of solid B_2H_6 (per valence electron) for a static-nuclei system, shown as a difference from that of the $P2_1/m$ structure. The enthalpy of a decomposed system consisting of B and H phases is also presented, where the α - B_{12} ($R\bar{3}m$)²⁶, γ - B_{28} ($Pnnm$)²⁷, and α -Ga ($Cmca$)²⁸ structures are considered for B phase, and the $Pca2_1$ ²⁹, $C2/c$ ³⁰, $Cmca$ -12³⁰, $Cmca$ ³¹, and Cs-IV ($I4_1/amd$)³² structures for H phase.

beyond 350 GPa; its structure is $Pbcn$. Possible stabilization against disproportionation at high pressures was previously pointed out by Barbee *et al.*³⁴ for BH_3 , though the structures for B, H, and BH_3 selected by them have a somewhat higher enthalpy. Even for Group-14 hydrides, similar tendencies for elemental separation has also been predicted^{5,35}. Despite the instability below 350 GPa, it is also worth mentioning that all the above structures have neither isolated protons nor proton pairs; instead, every proton appears to be closely attached to B ions³³. This implies that these B_2H_6 structures, some of which are even metallic, may exist as metastable phase below 350 GPa.

The densities of states per valence electron of the $P2_1/c$, $Pna2_1$, $P2_1/m$, and $Pbcn$ structures are shown at selected pressures in Fig. 2 the lower energy regions generally displaying a nearly free electron character. While the $P2_1/c$ structure is semiconducting, the other three

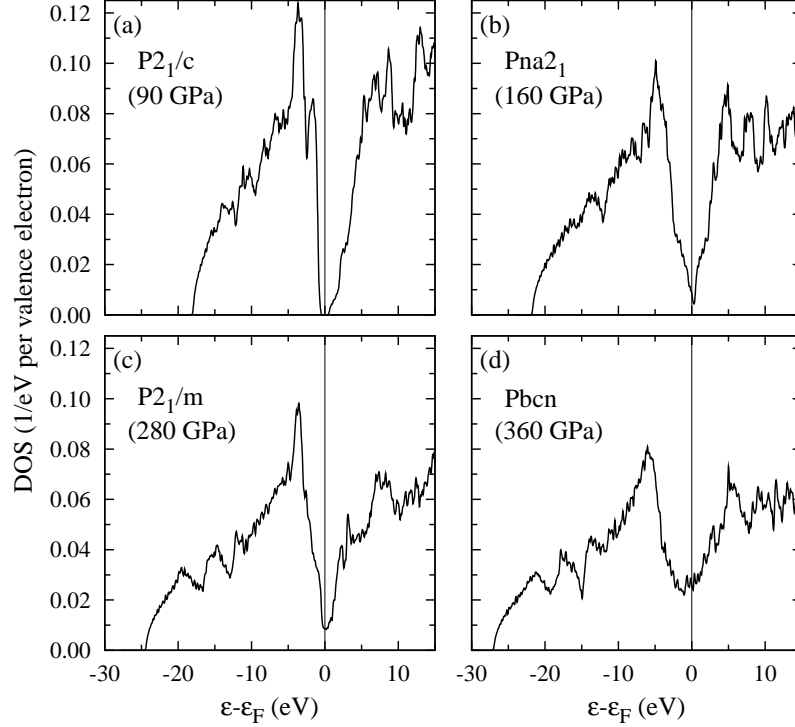


FIG. 2: The densities of states of (a) the $P2_1/c$ structure at $r_s = 1.5$, (b) the $Pna2_1$ structure at $r_s = 1.4$, (c) the $P2_1/m$ structure at $r_s = 1.31$, and (d) the $Pbcn$ structure at $r_s = 1.27$.

structures are metallic. Within the GGA, band-overlap metallization appears to take place at 120 GPa, in the $Pna2_1$ phase. The extent of the band overlap, however, does not increase greatly as pressure is increased, and even at 220 GPa is just 1.2 eV. Since the bandgap is well known to be underestimated in the GGA, the actual metallization might happen only after transition into the $P2_1/m$ phase, where significant band crossing is found. But a remarkable finding here is that in the $Pbcn$ phase, the density of states at the Fermi energy is notably high. In addition, the electronic states near the Fermi surface seem to be well delocalized since there is no evidence of sharp peak in the density of states in the vicinity of the Fermi energy. Given that we are dealing here with light elements with high dynamic energies the consequences of this for superconductivity are interesting, a matter we take up below.

The structure of the $Pbcn$ phase is shown in the top panels of Fig. 3. One can no longer identify a molecular-like picture which, as a matter of fact, is already lost at lower pressures in the $Pna2_1$ phase³³. Every proton now bridges two B ions, forming a B-H-B bond and the network of B-H-B bonds then make up a plane, where a nearly hexagonal arrangement of atoms can be observed. Subsequently each plane is connected to its neighboring planes

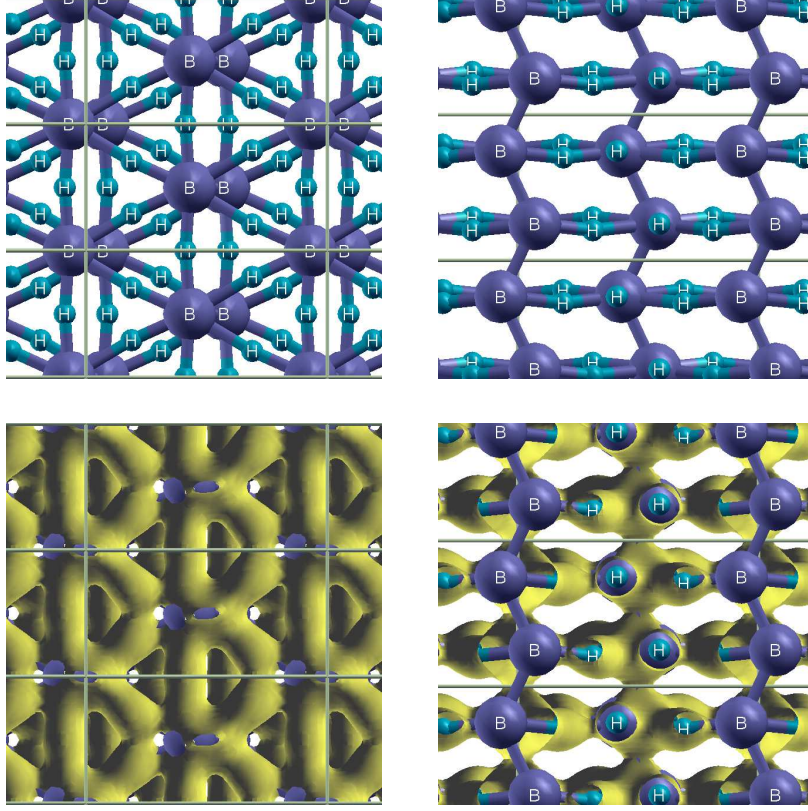


FIG. 3: (color online). The top and side views of the *Pbcn* structure at $r_s = 1.27$ (360 GPa) (top panels), and its partial electron density (bottom panels). The partial electron density is constructed from the Kohn-Sham states whose energy lies between $\varepsilon_F - 0.5$ eV and $\varepsilon_F + 0.5$ eV. The isosurface is taken for the average value, 0.0232 \AA^{-3} .

through zig-zag B-B bonds. Though the structure has planar character, the electronic state remains notably three dimensional as revealed in the density of states (Fig. 2(d)). It is interesting to note that analogous properties are also predicted for SiH_4 ⁷ and PbH_4 ³⁵. The partial electron density, which is constructed from the states near the Fermi energy, is presented in the bottom panels of Fig. 3, where an isosurface is taken for the average value. The partial density is found to be delocalized through the B-H-B and B-B bonds and is higher around the B-H-B bonds than around the B-B bonds. Thus, the electronic states near the Fermi surface have significant overlap with the protons which, importantly, indicates that electrons around the Fermi energy may undergo crucial interactions with the protons and, in turn, with any associated high-frequency phonons.

For the *Pbcn* structure, we have carried out frozen phonon calculations with the Phonopy

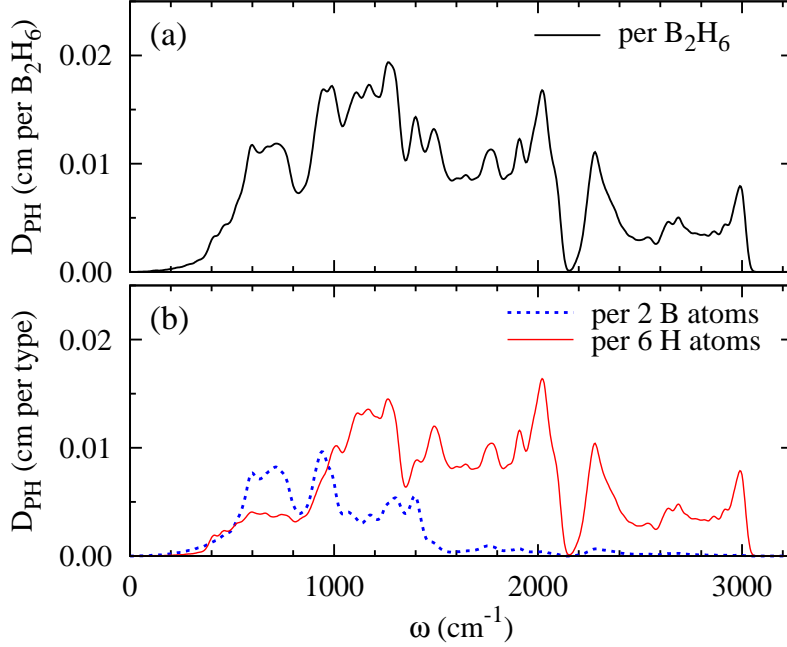


FIG. 4: (color online). The density of phonon modes (D_{PH}) of *Pbcn* structure at $r_s = 1.27$ (360 GPa): (a) total value (per B_2H_6); (b) partial value (summed in each atomic type).

code³⁶, by using a $2 \times 2 \times 2$ supercell containing 128 atoms. The resulting total and partial densities of phonon modes are presented in Fig. 4. The density of phonon modes shows a clear ω^2 dependence at small ω , and no imaginary frequency modes are found. Hence, the *Pbcn* structure is stable within the harmonic approximation. Also, notice that the maximum frequency is fairly high as mentioned earlier. In fact it reaches $\sim 3000 \text{ cm}^{-1}$ (0.37 eV), and this value is comparable to that of the Raman active vibron (pair stretching mode) observed in solid hydrogen at $\sim 320 \text{ GPa}$ ¹¹. The high frequency modes are attributed almost entirely to the motions of protons, as seen in Fig. 4(b). In particular, the modes from 2200 to 3000 cm^{-1} have motions such that protons are displaced along the B-H-B bonds within each plane. From the density of phonon modes we can determine the average zero point energy (ZPE) per formula unit (B_2H_6) and per valence electron; these are, respectively, 2.21 eV and 0.184 eV.

The above key findings in the *Pbcn* structure, namely, the large density of states at the Fermi energy, the significant overlap of partial electron density on the protons, and the high average energy of the phonons, all suggest that the *Pbcn* phase may exhibit fairly high temperature superconductivity. To examine this point further, we have estimated T_c using

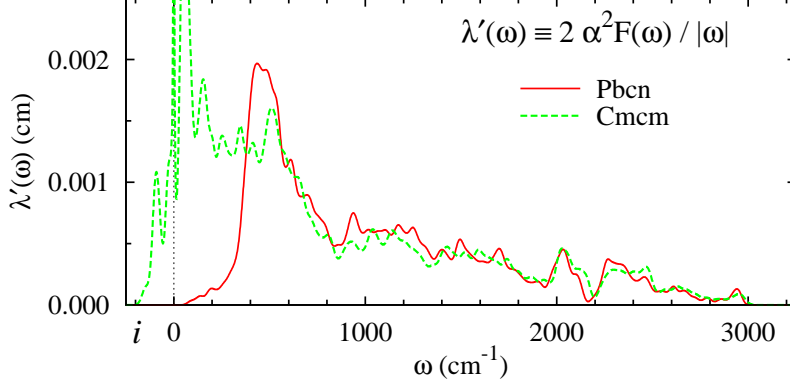


FIG. 5: (color online). The integrand of λ (i.e. $\lambda'(\omega) \equiv 2\alpha^2 F(\omega)/|\omega|$) of the *Pbcn* and *Cmcm* structures at $r_s = 1.27$ (360 GPa). In the abscissa, the region below zero means that the frequency is imaginary.

the standard McMillan formula³⁷ along with the Allen-Dynes corrections³⁸. The electron-phonon coupling is analyzed within DFPT, and we have used the ABINIT package³⁹ for this purpose. In the computations, a norm-conserving pseudopotential is utilized, where the cutoff radii for B and H are 0.89 and 0.68 Å, respectively, and the cutoff energy is set to 1224 eV. The number of \mathbf{k} -points is taken to be $10 \times 20 \times 16$ for the orthorhombic cell with $a=4.588$ Å, $b=2.405$ Å, and $c=2.765$ Å. With the Coulomb parameter set, for example, to $\mu^* = 0.13$, the estimated T_c is about 125 K at 360 GPa. Since there is uncertainty in the choice of μ^* , we have also examined the dependence of T_c on μ^* and it appears that even if μ^* is increased to 0.2, T_c still reaches 90 K. (As a guide, the dependence of T_c on μ^* is shown in Ref. 33). The electron-phonon interaction parameter is $\lambda = 1.32$ and the logarithmic average phonon frequency is $\omega_{\log} = 1270$ K. The λ is seen to be rather large, being just a little smaller than that of lead ($\lambda = 1.55$)³⁸. Yet, the T_c of the *Pbcn* is much higher than that of lead (7.2 K) mainly, of course, as a consequence of the quite large ω_{\log} .

Figure 5 shows the integrand of λ , namely, $\lambda'(\omega) \equiv 2\alpha^2 F(\omega)/\omega$, where $\alpha^2 F(\omega)$ is the Eliashberg spectral function. In the *Pbcn* structure, there exist no soft phonon modes which can cause drastic increases of $\lambda'(\omega)$ at small ω . Put in other terms, the fairly large λ in the *Pbcn* structure arises from the entire spectrum of $\lambda'(\omega)$. Indeed, chiefly due to the large density of states at the Fermi energy, the size of $\lambda'(\omega)$ is appreciable over a wide range of frequency (though it inevitably decays at higher frequency because of the factor of $1/\omega$). This character of $\lambda'(\omega)$ is thus favorable for achieving high ω_{\log} with λ kept large. Actually,

$\lambda'(\omega)$ is the weight function for obtaining $\langle \log \omega \rangle$, namely, $\langle \log \omega \rangle = \int d\omega \log \omega \cdot \lambda'(\omega) / \lambda$. In the *Pbcn* structure, the decay of $\lambda'(\omega)$ below 400 cm^{-1} and the persistence of $\lambda'(\omega)$ up to 3000 cm^{-1} attributable to the high-frequency phonons thus lessen the weight at low frequencies and helps raise ω_{\log} .

At this point we now turn to the *Cmcm* structure, whose enthalpy is fairly close to that of *Pbcn* (Fig. 1). The *Cmcm* structure is very similar to the *Pbcn* structure, and is likewise highly metallic. But in fact, at the harmonic level the *Cmcm* structure has a phonon mode with imaginary frequency at the zone boundary, and the consequent unstable motion then leads to the eventual distortion into the *Pbcn* structure³³. The magnitude of the imaginary frequencies is at most $\sim 250 \text{ cm}^{-1}$ at 360 GPa, and hence not so substantial given the light mass of hydrogen and its much higher modes. It means that a possible stabilization of the *Cmcm* structure originating with anharmonicity cannot be ruled out, if the even order anharmonicities are particularly significant (in which case the self-consistent harmonic approximation may be a plausible alternative). In Fig. 5, the $\lambda'(\omega)$ of the *Cmcm* structure is also shown. The impending instability within the harmonic approximation causes $\lambda'(\omega)$ to grow drastically around $\omega = 0$, and this behavior usually results in a considerably diminished ω_{\log} . However, it is interesting to note that the $\lambda'(\omega)$ is otherwise very similar to that of the *Pbcn* structure beyond 500 cm^{-1} . If the instability is indeed removed by anharmonicity, and consequently $\lambda'(\omega)$ at low frequencies is lessened, the *Cmcm* structure could also possess the same scale of T_c as that of the *Pbcn* structure.

Lastly, we return to the likely effects of ion dynamics on the location of the phase transition around 350 GPa. As noted above, we have estimated the ZPE from the frozen phonon calculations within the harmonic approximation. The ZPEs of the *P2₁/m* and *Pbcn* structures at 350 GPa are 0.183 and 0.184 eV per valence electron (2.20 and 2.21 eV per B_2H_6), respectively, and are thus significant. Since the difference between the two is rather small, however, the transition pressure from the *P2₁/m* structure to the *Pbcn* structure is not greatly affected by considering the ZPE. We have also examined the ZPE regarding B (*Cmca*) phase and H (*Cmca*) phase at 350 GPa. The ZPEs of the B and H phases are 0.069 and 0.309 eV per valence electron, respectively. The ZPE of the decomposed system (B+H) is then 0.189 eV per valence electron, which is 0.005 eV higher than that of the *Pbcn* structures. Hence, the pressure of thermodynamic stabilization of the *Pbcn* structure should not be notably raised even if the ZPE is considered.

By way of summary, we have investigated crystalline B_2H_6 at high pressures using density functional theory. Our results suggest that B_2H_6 becomes stable against separation into elemental B and H beyond 350 GPa, though metastable (metallic) phase may exist at pressures below this. The proposed candidate structure is the $Pbcn$ structure there, but possibly the $Cmcm$ structure if the anharmonicity is significant. In both of the structures, the density of states at the Fermi energy is large, the average phonon energy is high (the ZPE reaching 2.2 eV per B_2H_6), and the contribution of states associated with hydrogen to the overall states near the Fermi energy is substantial. By way of an estimate we have also examined the superconducting transition temperature from McMillan's formula with Allen-Dynes correction. The estimated T_c in the $Pbcn$ phase is characteristically of the size of 100 K, which is rather high for superconductivity driven by electron-phonon coupling. The pressure of the transition into the $Pbcn$ or $Cmcm$ structure is indeed high (350 GPa), but it may be noted that this pressure is close to the current capability of diamond anvil cells.

We have mentioned earlier the comparison of B_2H_6 with NH_3 , both under compression. It may also be useful to point out that there exists an intermediate system, namely $BH_3 \cdot NH_3$ (which necessarily has a permanent dipole moment) and this is presently under investigation with respect to its high pressure properties. Currently the metal with the lowest melting point (~ 78 K) is $Li(NH_3)_4$ the addition of Li to NH_3 lowering the melting point of ammonia by about 100 K. The fact that ammonia takes up lithium so easily might well be related to its permanent dipole moment, something B_2H_6 lacks. Nevertheless it might be of interest to examine possible stoichiometric additions of Li to B_2H_6 particularly we suggest, at high pressures. (The melting point of B_2H_6 is much lower than that of NH_3). Similar suggestions might then be raised for Li additions to $BH_3 \cdot NH_3$, which as noted above, does possess a dipole moment.

We thank Prof R. Hoffmann and his group, and Dr Y. Yao for helpful discussions. This work was supported in part by the National Science Foundation under Grant DMR 0907425.

¹ J. J. Gilman, Phys. Rev. Lett. **26**, 546 (1971).

² N. W. Ashcroft, J. Phys.: Condens. Matter **16**, S945 (2004).

- ³ N. W. Ashcroft, Phys. Rev. Lett. **92**, 187002 (2004).
- ⁴ J. Feng, W. Grochala, T. Jaron, R. Hoffmann, A. Bergara, and N. W. Ashcroft, Phys. Rev. Lett. **96**, 017006 (2006).
- ⁵ C. J. Pickard and R. J. Needs, Phys. Rev. Lett. **97**, 045504 (2006).
- ⁶ Y. Yao, J. S. Tse, Y. Ma, and K. Tanaka, Eur. Phys. Lett. **78**, 37003 (2007).
- ⁷ M. Martinez-Canales, A. R. Oganov, Y. Ma, Y. Yan, A. O. Lyakhov, and A. Bergara, Phys. Rev. Lett. **102**, 087005 (2009).
- ⁸ L. Sun, A. L. Ruoff, C.-S. Zha, and G. Stupian, J. Phys.: Condens. Matter **18**, 8573 (2006).
- ⁹ M. I. Erements, I. A. Trojan, S. A. Medvedev, J. S. Tse, and Y. Yao, Science **319**, 1506 (2008).
- ¹⁰ T. A. Strobel, A. F. Goncharov, C. T. Seagle, Z. Liu, M. Somayazulu, V. V. Struzhkin, and R. J. Hemley, Phys. Rev. B **83**, 144102 (2011).
- ¹¹ P. Loubeyre, F. Occelli, and R. LeToullec, Nature (London) **416**, 613 (2002).
- ¹² A. F. Goncharov and E. Gregoryanz and R. J. Hemley and H. K. Mao, PNAS **98**, 14234 (2001).
- ¹³ C. Narayana, H. Luo, J. Orloff, A. L. Ruoff, Nature (London) **393**, 46 (1998).
- ¹⁴ N. W. Ashcroft, Phys. Rev. Lett. **21**, 1748 (1968).
- ¹⁵ L. Sun, Z. Zhao, A. L. Ruoff, C.-S. Zha, and G. Stupian, J. Phys.: Condens. Matter **19**, 425206 (2007).
- ¹⁶ L. Sun, A. L. Ruoff, C.-S. Zha, and G. Stupian, J. Phys. Chem. Solids **67**, 2603 (2006).
- ¹⁷ C. J. Pickard and R. J. Needs, Nature Materials **7**, 775 (2008).
- ¹⁸ Y. Song, C. Murli, and Z. Liu, J. Chem. Phys. **131**, 174506 (2009); C. Murli and Y. Song, J. Phys. Chem. B **113**, 13509 (2009).
- ¹⁹ W. H. Eberhardt, B. Crawford Jr., and W. N. Lipscomb, J. Chem. Phys. **22**, 989 (1954).
- ²⁰ R. Hoffmann and W. N. Lipscomb, J. Chem. Phys. **37**, 2872 (1962).
- ²¹ K. F. Herzfeld, Phys. Rev. **29**, 701 (1927).
- ²² S. Baroni, S. de Gironcoli, A. Dal Corso, and P. Giannozzi, Rev. Mod. Phys. **73**, 515 (2001).
- ²³ J. P. Perdew, in *Electronic Structure of Solids '91*, edited by P. Ziesche and H. Eschrig (Akademie Verlag, Berlin, 1991), p. 11; J. P. Perdew, K. Burke, and M. Ernzerhof, Phys. Rev. Lett. **77**, 3865 (1996).
- ²⁴ P. E. Blöchl, Phys. Rev. B **50**, 17953 (1994); G. Kresse and D. Joubert, Phys. Rev. B **59**, 1758 (1999).
- ²⁵ G. Kresse and J. Hafner, Phys. Rev. B **47**, R558 (1993); **49**, 14251 (1994); G. Kresse and J.

- Furthmüller, Comput. Mat. Sci. **6**, 15 (1996); G. Kresse and J. Furthmüller, Phys. Rev. B **54**, 11169 (1996).
- ²⁶ B. F. Decker and J. S. Kasper, Acta Crystallogr. **12**, 503 (1959).
- ²⁷ A. R. Oganov, J. H. Chen, C. Gatti, Y. Z. Ma, Y. M. Ma, C. W. Glass, Z. X. Liu, T. Yu, O. O. Kurakevych, V. L. Solozhenko, Nature (LONDON) **457**, 863 (2009).
- ²⁸ U. Häussermann, S. I. Simak, R. Ahuja, B. Johansson, Phys. Rev. Lett. **90**, 065701 (2003).
- ²⁹ H. Nagara and T. Nakamura, Phys. Rev. Lett. **68**, 2468 (1992);
- ³⁰ C. J. Pickard and R. J. Needs, Nature Physics **3**, 473 (2007);
- ³¹ B. Edwards, N. W. Ashcroft, and T. Lenosky, Europhys. Lett. **34**, 519 (1996);
- ³² K. Nagao, H. Nagara, and S. Matsubara, Phys. Rev. B **56**, 2295 (1997).
- ³³ See supplementary material at XXXXX for more detailed data on structures and McMillan T_c .
- ³⁴ T. W. Barbee III, A. K. McMahan, and J. E. Klepeis, Phys. Rev. B **56**, 5148 (1997).
- ³⁵ P. Zeleski-Ejgierd, R. Hoffmann, and N. W. Ashcroft, Phys. Rev. Lett. **107**, 037002 (2011).
- ³⁶ Atsushi Togo, Fumiyasu Oba, and Isao Tanaka, Phys. Rev. B **78**, 134106 (2008).
- ³⁷ W. L. McMillan, Phys. Rev. **167**, 331 (1968).
- ³⁸ P. B. Allen and R. C. Dynes, Phys. Rev. B **12**, 905 (1975).
- ³⁹ X. Gonze, J.-M. Beuken, R. Caracas, F. Detraux, M. Fuchs, G.-M. Rignanese, L. Sindic, M. Verstraete, G. Zerah, F. Jollet, M. Torrent, A. Roy, M. Mikami, Ph. Ghosez, J.-Y. Raty, and D. C. Allan, Comput. Mater. Sci. **25**, 478 (2002).